Indian Journal of Pure & Applied Physics
Vol. 58, April 2020, pp. 271-276

Gamma, X-ray and neutron shielding properties of boron polymers

N Nagaraja[a,b], H C Manjunatha[c*], L Seenappa[c], K V Sathish[c], K N Sridhar[a,b] & H B Ramalingam[d]

[a]Department of Physics, Government First Grade College, Kolar 563 101, India

[b]Research and Development Centre, Bharathiar University, Coimbatore 641 046, India

[c]Department of Physics, Government College for Women, Kolar 563 101, India

[d]Department of Physics, Government Arts College, Udumalpet 642 126, India

Received 17 February 2020

We have studied the X-ray and gamma radiation shielding parameters such as mass attenuation coefficient, linear attenuation coefficient, Half Value Layer (HVL), Tenth Value Layer (TVL), effective atomic number and electron density in some boron polymers of different boron based polymers [Polymer A-PolyBorazylene ($B_3N_3H_4$), Polymer B- 4-Vinylphenyl Boronic acid ($C_8H_9O_2B$), Polymer C- Borazine ($B_3N_3H_6$), Polymer D- 3-Acrylamidophenylboronic acid ($C_9H_{10}BNO_3$) Polymer E-Phenylethenylboronic acid ($C_{14}H_{19}BO_2$), Polymer F- 4-Aminophenylboronic acid ($C_{12}H_{18}BNO_2$) and Polymer G- 3- Aminophenylboronic acid ($C_6H_8BNO_2$)]. We have also studied the neutron shielding properties such as coherent neutron scattering length, incoherent neutron scattering lengths, coherent neutron scattering cross section, incoherent neutron scattering cross sections, total neutron scattering cross section and neutron absorption cross sections in the boron polymers. We have compared the shielding properties among the studied different boron polymers. From the detail study, it is clear that the boron polymer Phenylethenylboronic acid is good absorber for X-ray, gamma radiation and neutron. Hence, we suggest that the boron polymer Phenylethenylboronic acid is good shielding material for X-ray, gamma and neutrons.

Keywords: Radiation shielding, Boron based polymers, Mass attenuation coefficients

1 Introduction

It is necessary to search for new radiation shielding materials to replace more toxic and dense shielding materials such as lead. The mass attenuation coefficient and its derivables are basic parameters in the selection of shielding materials for X-ray and gamma radiation. Singh and Badiger[1] studied the gamma and neutron shielding properties of some alloy materials. Mann[2] studied gamma ray shielding behaviors of some nuclear engineering materials. Singh and Badiger[3] computed the gamma-ray interaction characteristics of some boron containing materials by means of effective atomic numbers and exposure buildup factors. Badawy and Abd Latif [4] studied the synthesis and characterizations of magnetite nanocomposite films for radiation shielding. Sayyed[5] studied the gamma and neutron shielding properties of eight different types of smart polymers. Mann *et al*.[6] studied the shielding behaviors of some polymer and plastic materials for gamma-rays in the experimental energy range 10–1400 keV. Seenappa *et al*.[7] studied the gamma, X-ray and neutron shielding properties of polymer concretes. Gurler and Tarim[8] determined the radiation shielding properties of some polymer and plastic materials against gamma-rays. Srinivasan and Samuel[9] studied the evaluation of radiation shielding properties of the polyvinyl alcohol/iron oxide polymer composite. Manjunatha and Seenappa[10] studied the X-ray and gamma radiation shielding parameters Gamma, X-ray and neutron radiation shielding properties of aluminium polymer concrete, silicon polymer concrete, potassium polymer concrete, sodium polymer concrete, boron polymer concrete and lead polymer concrete. Pavlenko *et al*.[11] studied the radiation shielding composites based on polyimide and surface and physical-mechanical properties of polyimide/Bi_2O_3 composites.

In the present work, we have studied the X-ray, gamma and neutron radiation shielding parameters such as mass attenuation coefficient, linear attenuation coefficient, Half Value Layer (HVL), Tenth Value Layer (TVL), effective atomic number and electron density in some boron polymers of different composition such as Polymer A-Poly Borazylene ($B_3N_3H_4$) [0.81gm/cm^3], Polymer B- 4-

*Corresponding author (E-mail: manjunathhc@rediffmail.com)

Vinylphenyl Boronic acid ($C_8H_9O_2B$) [1.09gm/cm^3], Polymer C- Borazine ($B_3N_3H_6$) [0.81 gm/cm^3], Polymer D- 3-Acrylamidophenylboronic acid ($C_9H_{10}BNO_3$) [1.2gm/cm^3]. Polymer E- Phenyl-ethenylboronic acid ($C_{14}H_{19}BO_2$) [1.13gm/cm^3], Polymer F- 4-Aminophenylboronic acid ($C_{12}H_{18}BNO_2$) [1.23gm/cm^3] and Polymer G- 3- Aminophenylboronic acid ($C_6H_8BNO_2$) [1.21gm/cm^3]. We have also studied the neutron shielding properties such as coherent neutron scattering length, incoherent neutron scattering lengths, coherent neutron scattering cross section, incoherent neutron scattering cross sections, total neutron scattering cross section and neutron absorption cross sections in the boron polymers.

2 Theory

2.1 Gamma/X-ray interaction parameters

A narrow beam of mono-energetic photons is attenuated to an intensity I from an incident intensity I_0 in passing through a layer of material with mass-per-unit-area x according to the exponential absorption law:

$$\frac{I}{I_0} = \exp\left(-\mu/\rho \cdot x\right) \quad \ldots (1)$$

In which μ/ρ is the mass attenuation coefficient (MAC) and equation (1) can be rewritten as:

$$\frac{\mu}{\rho} = \frac{1}{x}\ln\left(\frac{I_0}{I}\right) \quad \ldots (2)$$

μ/ρ is related to the total cross section (area) per atom $\sigma_{tot:}$

$$\frac{\mu}{\rho} = \sigma_{tot}\left(N_A/A_r\right) \quad \ldots (3)$$

In which N_A is avagadro's number (6.022045×10^{23} mol^{-1}) and A_r is the relative atomic mass (atomic weight). The total cross section σ_{tot}, in turn, can be written as the sum over contributions from the principal photon interactions:

$$\sigma_{tot} = \sigma_{coh} + \sigma_{incoh} + \tau + \kappa + \sigma_{ph.n.} \quad \ldots (4)$$

In which σ_{coh} and σ_{incoh} are the coherent (Rayleigh) and incoherent (Compton) scattering cross sections, respectively; τ is the atomic photo effect cross section; κ is the positron-electron pair-production (including triplet) cross section; and $\sigma_{ph.n.}$ is the photonuclear cross section [12-14].

Thus The μ/ρ can be expressed in terms of the cross sections as fallows:

$$\mu/\rho = \left(N_A/A_r\right)\left(\sigma_{coh} + \sigma_{incoh} + \tau + \kappa\right) \quad \ldots (5)$$

In the mass attenuation coefficients (MAC) and photon interaction cross sections in the energy range from 1 keV to 100 GeV are generated using WinXCom[15]. In this code, σ_{coh} and σ_{incoh} were adopted from Hubbell and Overbo[12] and Hubbell *et al.*[13] respectively. Values of τ and *κ* are adopted from Scofield[14] which involves relativisitic Hartree-Fock renormalization factors.

The total linear attenuation coefficient (μ) can be evaluated by multiplying density of compounds to mass attenuation coefficients. The total linear attenuation coefficient (μ) is used in the calculation of Half Value Layer (HVL). HVL is the thickness of a interacting medium that reduces the radiation level by a factor of 2 that is to half the initial level and is calculated by the ratio of 0.693 to the linear attenuation coefficient. The total linear attenuation coefficient (μ) is also used in the calculation of Tenth Value Layer (TVL). It is the thickness of interacting medium for attenuating a radiation beam to 10% of its radiation level and is computed by the ratio of 2.303 to the linear attenuation coefficient. The average distance between two successive interactions is called the relaxation length (λ). It is also called the photon mean free path which is determined by the reciprocal of linear attenuation coefficient. The gamma interaction parameters such as linear attenuation coefficients μ(cm^{-1}), HVL (in cm), TVL (in cm) and mean free path λ are evaluated. The equivalent atomic number of a composite material that will produce the same effect as that of a single element when it interacts with photons is referred as equivalent atomic number. The effective atomic number is evaluated by taking the ratio between atomic cross section and electronic cross section. The procedure of evaluation of atomic and electronic cross section is explained in the previous work[16-18].The number of electrons per unit mass is referred as electron density. The effective electron density is derived from the evaluated effective atomic number. The procedure of evaluation of effective electron density is explained in the previous work[19-37].

2.2 Neutron shielding parameters

The neutron shielding properties (NSP) such as coherent neutron scattering length, incoherent neutron scattering lengths, coherent neutron scattering cross section, incoherent neutron scattering cross sections, total neutron scattering cross section and neutron

absorption cross sections in silicon boron alloys are calculated using mixture rule and available data for elements in the literature[38].

3 Experimental Details

We have conducted transmission experiments with the narrow beam geometry to measure the incident and transmitted intensities. The detail experimental arrangement is explained in the previous report[19]. Experimental arrangement is as shown in Fig. 1. We have used a NaI(Tl) crystal detector (2.54×2.54cm^2) mounted on a photomultiplier tube housed in a lead chamber with a sophisticated PC based MCA for a detection purpose. The given compound in a powder form is filled in circular perspex holder of 1cm diameter and a standard thickness of 1 cm. The compound was directly attached to the opening of the lead shield in which the source was placed.

The gamma sources such as ^{170}Tm (0.084 MeV) [2.1mCi], ^{137}Cs (0.662 MeV) [3.14mCi] and ^{60}Co (1.170, 1.330 MeV)[3.16mCi] are used. For a point source located along the axis of a right circular cylindrical detector the solid angle can be written as:

$$\Omega = 2\pi\left[1-\frac{1}{\left[1+(a/d)^2\right]^{1/2}}\right] \quad \ldots (6)$$

where a is the radius of the detector and d = r+x, where r is the source to detector distance and 'x ' is the mean depth of interaction with in the detector . For d ≫ a the solid angle becomes:

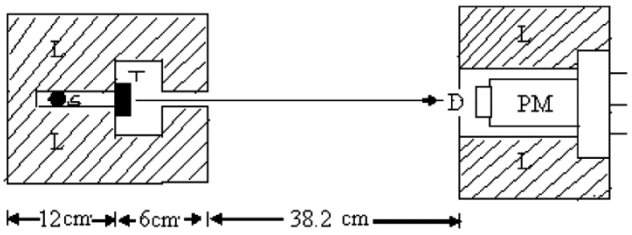

Fig. 1 — Experimental setup for the measurement of (μ/ρ) [S-Source Position, T-Target sample, L-Lead Shielding, D-Detector, PM-Photomultiplier]

$$\Omega = \pi a^2/d^2 \quad \ldots (7)$$

The studied polymers are used as target samples. The sample was directly attached to the opening of the lead shield where source is placed. The integral intensities, I_0 and I of the beam before and after passing through the sample are measured for sufficient time. (μ/ρ)c of the sample is then estimated using the relation:

$$\left(\frac{\mu}{\rho}\right)_c = \left(\frac{1}{t\rho}\right) ln\left(\frac{I_0}{I}\right) \quad \ldots (8)$$

Experimental values of Nel and Zeff of polymers were obtained from (μ/ρ)c using the procedure explained in our previous work[19]. The errors in the present measurements are mainly due to counting statistics, non uniformity of the absorber, impurity content of the samples, and scattered photons reaching the detector. These errors are attributed to the deviation from the average value in the I and I_0 (<3.3%), sample thickness (<0.7%), the mass of sample (<0.2%), and systematic errors (<0.8%). Also, the ratio of theoretical (T) and experimental (E) values is ≤1.1%. The maximum errors in the mass attenuation coefficients have been calculated from errors in incident (I_0) and transmitted (I) intensities and areal density (t) by using the propagation of error formula:

$$\Delta\left(\frac{\mu}{\rho}\right) = \frac{1}{t}\sqrt{\left(\frac{\Delta I_0}{I_0}\right)^2 + \left(\frac{\Delta I}{I}\right)^2 + \left(\ln\frac{I_0}{I}\right)^2\left(\frac{\Delta t}{t}\right)^2} \quad \ldots (9)$$

where ΔI_0, ΔI and Δt are the errors in the intensities I_0, I and thickness t of the sample respectively.

4 Results and Discussion

The mass attenuation coefficients are compared with the theoretical values. This comparison is as shown in Table 1. The measured mass attenuation coefficients are used to calculate its derivable such as HVL, TVL, mean free path, Z_{eff} and N_{el}. Comparison of half value layer and tenth value layer among the

Table 1 — Comparison of experimental values of mass attenuation coefficient (μ/ρ) with theoretical values for different polymers

Polymer	84 keV		662 keV		1170 keV		1330 keV	
	Expt.	Theory	Expt.	Theory	Expt.	Theory	Expt.	Theory
B3N3H4	1.51E-01±(5.21E-3)	1.54E-01	7.40E-02±(2.55E-3)	7.80E-02	5.80E-02±(2.00E-3)	5.90E-02	5.20E-02± (1.79E-3	5.76E-02
C8H9BO2	2.49E-01±(1.11E-2)	2.52E-01	1.25E-01± (5.56E-3)	1.25E-01	9.10E-02±(4.05E-3)	9.50E-02	9.40E-02± (4.18E-3)	9.10E-02
B3N3H6	1.58E-01±(4.98E-3)	1.62E-01	7.90E-02± (2.49E-3)	8.10E-02	5.70E-02± (1.80E-3)	6.10E-02	5.80E-02± (1.83E-3)	5.80E-02
C9H10BNO3	1.59E-01±(7.08E-3)	1.62E-01	7.80E-02± (3.47E-3)	8.10E-02	5.90E-02± (2.63E-3	6.20E-02	5.60E-02± (2.49E-3)	5.80E-02
C14H19BO2	1.59E-01±(3.90E-3)	1.59E-01	7.80E-02± (1.91E-3)	7.90E-02	5.80E-02± (1.42E-3)	6.10E-02	5.30E-02± (1.30E-3)	5.70E-02
C12H18BNO2	1.63E-01±(5.13E-3)	1.67E-01	8.10E-02± (2.55E-3)	8.30E-02	5.90E-02± (1.86E-3)	6.30E-02	5.50E-02± (1.73E-3)	5.90E-02
C6H8BNO2	1.59E-01±(5.80E-3)	1.63E-01	7.80E-02± (2.85E-3)	8.10E-02	5.90E-02± (2.15E-3)	6.20E-02	5.40E-02± (1.97E-3)	5.80E-02

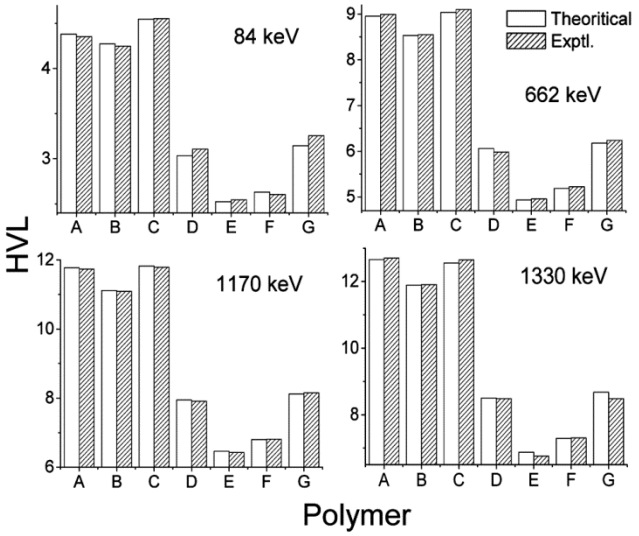

Fig. 2 — Comparison of half value layer (HVL) among the different studied polymers at different energies.

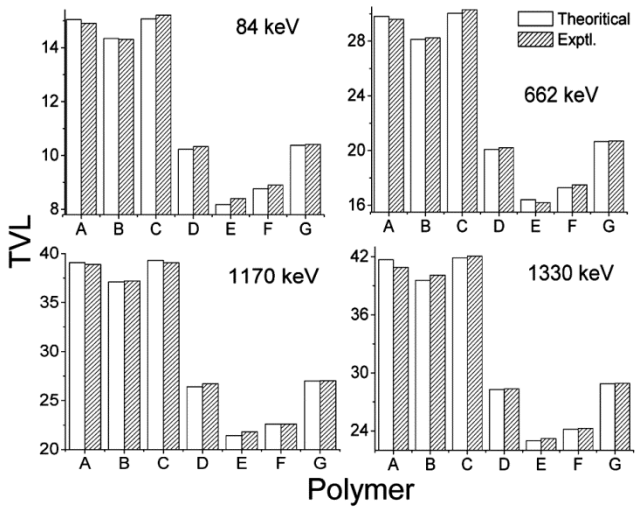

Fig. 3 — Comparison of tenth value layer (TVL) among the different studied polymers at different energies.

different studied polymers at different energies are as shown in Fig. 2 and 3. From this comparison, it is clear that the half value layer and tenth value layer are small for Phenylethenylboronic acid boron polymer than the other studied boron polymers. It means gamma/X-ray penetrates less in Phenylethenylboronic acid boron polymer than the other boron polymers. The comparison of mean free path (Theory and experimental) for different boron polymers is as shown in Fig. 4. From this comparison, it is clear that the mean free path is small for Phenylethenylboronic acid boron polymer than the other studied boron polymers. It means gamma/X-ray penetrates less in Phenylethenylboronic acid boron polymer than the

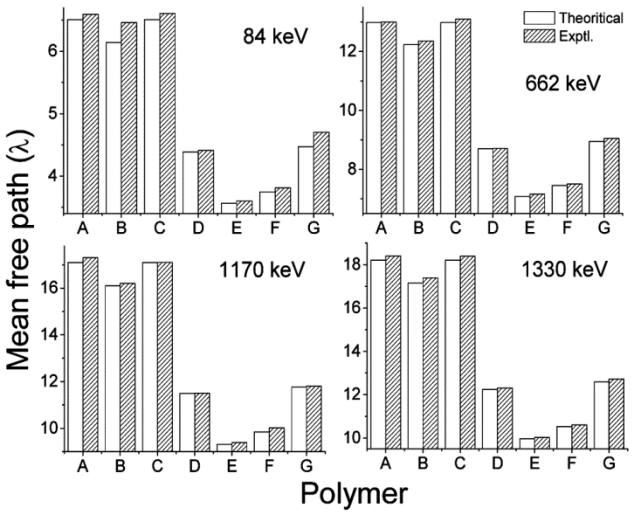

Fig. 4 — Comparison of mean free path (λ) among the different studied polymers at different energies.

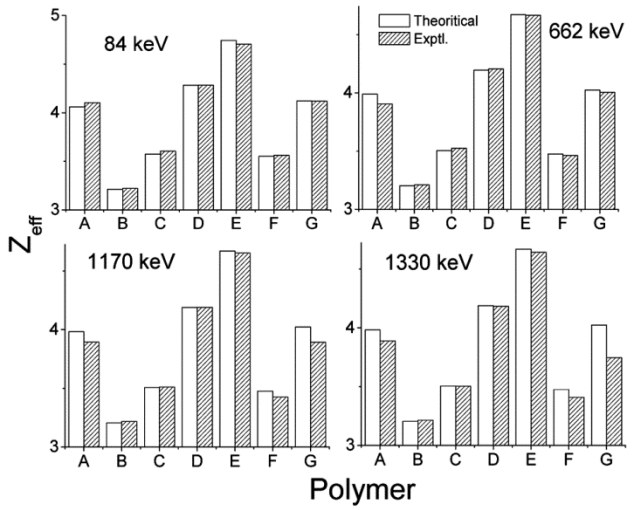

Fig. 5 — Comparison of effective atomic numbers (theoretical and experimental) among the different studied polymers at different energies.

other boron polymers. The comparison of effective atomic number among studied boron polymers at different energies are as shown in Fig. 5. The theoretical values are in good agreement with experimental values. From this comparison, it is clear that the effective atomic number is larger for Phenylethenylboronic acid boron polymer than the other studied boron polymers. The comparison of effective electron density at different energies for different boron polymers is as shown in Fig. 6. From this comparison, it is clear that the effective electron density is maximum for Phenylethenylboronic acid boron polymer than the other studied boron polymers.

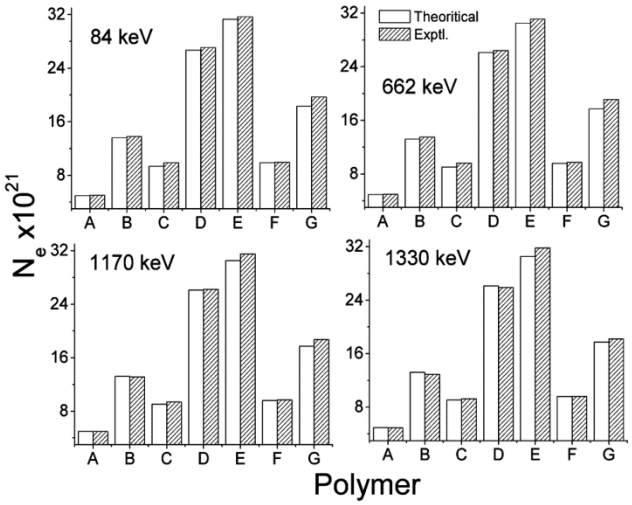

Fig. 6 — Comparison of effective electron density (theoretical and experimental) among the different studied polymers at different energies.

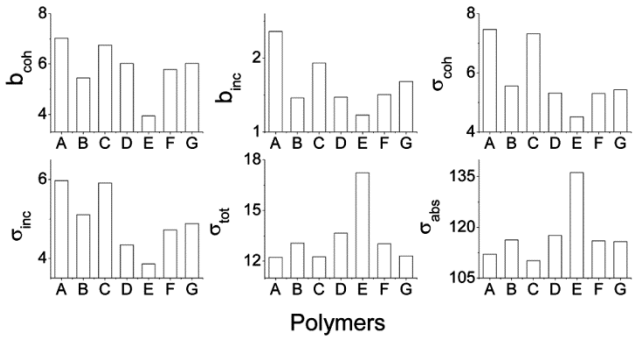

Fig. 7 — Comparison of neutron shielding parameters with different boron polymers (A-$B_3N_3H_4$, B-$C_8H_9BO_2$, C-$B_3N_3H_6$, D-$C_9H_{10}BNO_3$, E-$C_{14}H_{19}BO_2$, F-$C_{12}H_{18}BNO_2$ & G-$C_6H_8BNO_2$)

The comparison of evaluated coherent neutron scattering length, incoherent neutron scattering lengths, coherent neutron scattering cross section, incoherent neutron scattering cross sections, total neutron scattering cross section and neutron absorption cross sections for different boron polymers are as shown in Fig. 7. From this figure, it is clear that coherent neutron scattering length and incoherent neutron scattering lengths are minimum for Phenylethenylboronic acid boron polymer. Coherent and total neutron scattering cross sections are minimum for Phenylethenylboronic acid boron polymer. The neutron absorption cross section is high for Phenylethenylboronic acid boron polymer.

5 Conclusions

We have studied the X-ray, gamma and neutron shielding parameters in boron polymers. We have compared the experimental values with the theoretical values and from the comparison it is found that theoretical values are in good agreement with the experimental values. From this comparative study, it is clear that the boron polymer Phenylethenylboronic acid is good absorber for X-ray, gamma radiation and neutron. The attenuation parameters for neutron is large for boron polymer Phenylethenylboronic acid. Hence, we suggest that the boron polymer Phenylethenylboronic acid is good shielding material for X-ray, gamma and neutrons

References

1 Singh V P & Badiger N M, *Annal Nucl Energy*, 64 (2014) 301.

2 M K Singh, *Nucl Eng Technol*, 49 (2017) 792.

3 Singh V P & Badiger N M , *Vacuum*, 113 (2015) 24.

4 Badawy S M & Abd El-Latif A A , *Polymer Composites*, (2015), DOI 10.1002/pc.

5 Sayyed M I, *Chin J Phy*, 54 (2016) 408.

6 M K Singh, Rani A & H M Singh, *Radiat Phys Chem*, 106 (2015) 247.

7 Seenappa L, Manjunatha H C, Sridhar K N & Hanumantharayappa C, *Indian J Pure Appl Phys*, 56 (2018) 383.

8 Gurler O & Tarim U A, *Acta Phys Polonica A*, 130 (2016) 236.

9 K Srinivasan & E James Jabaseelan Samuel, *J Med Phys*, 42 (2017) 273.

10 Manjunatha H C & Seenappa L, *Int J Nucl Energy Sci Technol*, 12 (2018).

11 Pavlenko V I, Cherkashina N I & Yastrebinsky R N, Condensed Matter Phys, 5 (2019) e1703.

12 Hubbell J H & Overbo I, *J Phys Chem Ref Data*, 8 (1979) 69.

13 Hubbell J H, Veigele W M J, Briggs E A, Brown R T, Cromer D & Howerton R J, *J Phys Chem Ref Data*, 4 (1975) 471.

14 Scofield J H, Lawrence Livermore Lab Rep, UCRL-51326 (1973).

15 Gerward L, Guilbert N, Jensen K B & Levring H, *Radiat Phys Chem*, 71 (2004) 653.

16 Manjunatha H C, *Radiat Phys Chem*, 113 (2015) 24.

17 Seenappa L, Manjunatha H C, Chandrika B M & Hanumantharayappa C, J Radiat Prot Res, 42 (2017) 26.

18 Manjunatha H C, *Radiat Phys Chem*, 137(2016) 254.

19 Manjunatha H C & Seenappa L, Chandrika B M & Hanumantharayappa C, *Annal Nucl Energy*, 109 (2017) 310.

20 Rudraswamy B, Dhananjaya N & Manjunatha H C, *Nucl Insure Meth Phys Res A*, 619 (2010) 171.

21 Manjunatha H C, Chandrika B M, Seenappa L & Hanumantharayappa C, *Int J Nucl Energy Sci Technol*, 10 (2016) 356.

22 Manjunatha H C, *J Med Phys*, 39 (2014) 112.

23 Manjunatha H C, Chandrika B M, Rudraswamy B & Sankarshan B M, Nucl Instrum Meth Phys Res A, 674 (2012) 74.

24 Manjunatha H C & Rudraswamy B, *Health Phys*, 104 (2) (2013) 158.

25 Suresh K C, Manjunatha H C & Rudraswamy B, Radiat Protect Dosim, 128 (2008) 294.

26 Manjunatha H C & Rudraswamy B, Health Phys, 100 (2011) S92-S99.

27 Manjunatha H C & Rudraswamy B, Radiat Meas, 47 (2012) 364.

28 Manjunatha H C & Rudraswamy B, Radiat Phys Chem, 80 (2011) 14.

29 Manjunatha H C & Rudraswamy B, *J Radio Nucl Chem*, 294 (2012) 251.

30 Manjunatha H C, Seenappa L, Sridhar K N, Sowmya N & Hanumantharayappa C, *Eur Phys J D*, 71 (2017) 235.

31 Manjunatha H C, *Appl Radiat Isot*, 94 (2014) 282.

32 Manjunatha H C, Seenappa L, Sowmya N & Hanumantharayappa C, X-ray Spectrometry, 47 (2018) 34.

33 Manjunatha H C & Sridhar K N, *Nuclear Instrum Meth Phys Res A*, 877(2018) 349.

34 Seenappa L, Manjunatha H C, Sridhar K N & Hanumantharayappa C, *Nucl Sci Tech*, 29 (2018) 3.

35 Seenappa L, Manjunatha H C, Sridhar K N & Hanumantharayappa C, Int J Nucl Energy Sci Technol, 11 (2017) 377.

36 American National Standard (ANS), ANSI/ANS 6.4.3(1991).

37 Manjunatha H C, *Pramana J Phys*, 89:42.

38 Sears V F, *Neutron News*, 3(3), 26.

39 Hubbell J H, *At Data*, 3 (1971) 241.

40 Hubbell J H & Veigele W M, JNBS Publ. TN-901 (1976).

41 Gimm H A & Hubbell J H, NBS Publ. TN-968 (1978).